A STUDY OF PROVINCIAL CARBON EMISSIONS IN CHINA'S CONSTRUCTION INDUSTRY USING THE STIRPAT AND DEEP LEARNING MODEL

XU, W.[1] – ZHANG, C. L.[2] – REN, F.[3] – LIU, W. C.[4*] – WANG, W. Y.[5]

[1]*Logistics and Infrastructure Department, Sichuan Vocational College of Health and Rehabilitation, Zigong 643000, Sichuan Province, China*

[2]*The Chongqing Key Laboratory of Computational Intelligence, Chongqing University of Posts and Telecommunications, Chongqing 400065, China*

[3]*Department of Economics and Management, North China Electric Power University, Baoding 071003, Hebei Province, China*

[4]*School of Information Science and Engineering, Northeastern University, Shenyang 110000, Liaoning Province, China*

[5]*Huaneng Renewables Corporation Limited, Shaanxi Branch, Xi'an 710000, Shaanxi Province, China*

[*]*Corresponding author*
e-mail: ncepu_liuwencheng@126.com

(Received 11th Jun 2025; accepted 31st Jul 2025)

Abstract. The construction industry is a significant contributor to energy consumption and carbon emissions, making its decarbonization essential for achieving the "dual carbon" goals. However, existing studies often focus on national or single-region analyses and lack a systematic understanding of provincial-level disparities in emissions and peaking pathways. To address this challenge, this study first employs an extended STIRPAT (Stochastic Impacts by Regression on Population, Affluence, and Technology) model to identify nine key variables influencing carbon emissions, using data from the construction industry across 30 Chinese provinces from 1997 to 2021. Three scenarios—baseline, green development, and high-speed development—are developed for analysis. A novel forecasting model integrating Convolutional Neural Networks (CNN), Gated Recurrent Units (GRU), Long Short-Term Memory (LSTM) networks, and attention mechanisms is then proposed to predict the carbon emission trends and peaking timelines of China's construction sector from 2022 to 2035. The results indicate that the proposed model achieves higher prediction accuracy than traditional methods. Across all scenarios, carbon peaking targets are projected to be reached before 2030 in all provinces. The green development scenario results in faster emission reductions and earlier peaking, while the high-speed development scenario delays peaking in some central and western provinces, highlighting greater mitigation potential and spatial heterogeneity. Finally, policy recommendations based on the findings provide scientific guidance for the low-carbon transition of the construction industry and the formulation of province-specific emission reduction strategies by government authorities.
Keywords: *construction industry carbon emissions, deep learning, scenario analysis, carbon peaking, low-carbon development policies*

Introduction

The intensifying challenge of global climate change has driven nations worldwide to adopt low-carbon economic models as a shared developmental priority (Liu et al., 2023). In 2020, China announced its ambitious "dual carbon" goals: achieving carbon peaking by 2030 and carbon neutrality by 2060 (Li et al., 2023). This commitment was reinforced

http://www.aloki.hu ● ISSN 1589 1623 (Print) ● ISSN 1785 0037 (Online)
DOI: http://dx.doi.org/10.15666/aeer/2306_1075110774

in the 20th National Congress report, which emphasized the integrated advancement of "reducing carbon emissions, cutting pollution, expanding green development, and fostering growth" (Luo et al., 2025). As the second-largest source of carbon emissions after the industrial sector, the construction industry accounts for over 50% of China's total carbon emissions throughout its lifecycle (Xiao et al., 2023), making it a critical area for achieving carbon peaking and neutrality (Li et al., 2024).

In recent years, extensive research has been conducted on carbon emissions in the construction sector. These studies can be broadly categorized into two main areas: analyses of influencing factors (Yang et al., 2025) and carbon emission forecasting (Hu et al., 2023).

In terms of influencing factors, methods such as Grey Relational Analysis (Shaheen et al., 2023; Ding et al., 2023), STIRPAT (Wang et al., 2023; Cooray et al., 2023), LMDI (Li et al., 2023; Tian et al., 2023), and Kaya decomposition (Lin et al., 2023; Zhang et al., 2023) are commonly employed to investigate the driving or inhibitory effects of factors like economic growth, urbanization, and energy structure on carbon emissions.

Luo et al. (2023) used Kaya decomposition to analyze the inequality of CO2 emissions between urban and rural residents in China, dividing it into four contributing factors. Their findings revealed that, from 2005 to 2020, the per capita CO2 emissions of rural residents increased at a faster rate than that of urban residents. A dynamic decomposition further highlighted the varying characteristics of urban-rural disparity across different periods. Jiang et al. (2023) applied the LMDI model to examine the factors influencing carbon emission changes in China from 2008 to 2019, quantifying their contributions. Their results indicated that economic growth was the primary driver of increased carbon emissions. Zhou et al. (2023) analyzed carbon-related news themes reported by ABC and The Guardian from 2009 to 2019, constructing a global carbon emission transfer network. They extended the STIRPAT model to explore the direct and lagged effects of carbon-related news on emissions and transfers. Their findings showed that global attention to carbon issues intensified with increasing emissions, leading to policy recommendations for emissions reduction guided by media narratives. Zhang et al. (2023) employed the STIRPAT model to quantify the impact of urbanization on carbon emissions in the regional heating industry between 2012 and 2020. Their study demonstrated that urbanization effects on carbon emissions exhibit temporal and spatial heterogeneity, emphasizing the need for targeted clean heating policies to address the diverse impacts of urbanization, socioeconomic, and meteorological factors on emission reductions.

In terms of forecasting methods, the rise of machine learning and deep learning technologies has led to the widespread application of models such as LSTM (Jiang et al., 2024) and CNN (Chen et al., 2024) for short- and long-term carbon emission predictions, yielding promising results (Jin et al., 2024).

Zhou et al. (2024) proposed a predictive model combining Bidirectional LSTM and attention mechanisms for probabilistic daily carbon emission forecasting. Experimental results demonstrated that this model outperformed benchmark models in terms of metrics such as Mean Squared Error and Mean Absolute Error, enhancing the accuracy of daily carbon emission forecasts while providing policymakers with a robust tool for real-time monitoring and evaluation. Li et al. (2024) employed Monte Carlo simulations and an LSTM neural network to construct three scenarios for predicting the evolution of China's industrial carbon emissions from 2020 to 2030. Their analysis suggested that industrial carbon emissions in China are likely to peak before 2030, offering scientific support for developing low-carbon regulatory policies and achieving sustainable development.

http://www.aloki.hu ● ISSN 1589 1623 (Print) ● ISSN 1785 0037 (Online)
DOI: http://dx.doi.org/10.15666/aeer/2306_1075110774

Giannelos et al. (2024), acknowledging the construction sector's role in accounting for approximately 50% of global energy-related CO2 emissions, proposed and compared various machine learning-based methods to forecast the long-term carbon emission trends of the sector through 2050. Zheng et al. (2024) applied machine learning algorithms to predict the lifecycle carbon emissions of buildings. By modeling data from 150 typical residential buildings in Cornwall, UK, Zheng tested ten algorithms, including Multiple Linear Regression, Decision Trees, and Random Forests. The results confirmed the predictive capabilities of all tested algorithms, providing valuable insights for the application of lifecycle carbon emission research during the early design stages of construction projects.

However, existing studies primarily focus on national or regional total carbon emissions from the construction industry, with limited attention to detailed provincial-level analyses of future carbon peaking pathways. This gap hampers the development of comprehensive and balanced carbon reduction policies by governments. Additionally, traditional forecasting models struggle to address the complex volatility and temporal dependencies inherent in construction carbon emission data, limiting their ability to simultaneously extract spatial and temporal features effectively.

To address these limitations, this study leverages data from 30 Chinese provinces and proposes a hybrid predictive model integrating CNN, GRU, LSTM networks, and an attention mechanism (CNN-GRU-LSTM-Attention). The CNN component captures the spatial features of provincial data, while the GRU and LSTM modules model short- and long-term sequence dependencies, respectively. The attention mechanism further enhances the model by assigning higher weights to critical features, significantly improving prediction accuracy. This model enables government agencies and enterprises to gain a comprehensive understanding of regional carbon emission dynamics in the construction industry, scientifically plan the carbon peaking process, and provide quantitative decision-making support for achieving low-carbon and high-quality development in the sector.

The main contributions of this study are as follows:

1. While most existing research focuses on carbon emission forecasting for China as a whole or for single regions, this study delves into the differentiated characteristics and peaking pathways of carbon emissions at the provincial level. By analyzing and predicting carbon emissions in the construction industry across 30 provinces, this study provides a detailed depiction of regional disparities and their future trends. Combined with scenario analysis, the findings offer scientific guidance for precise carbon reduction strategies and the formulation of region-specific policies.

2. To address the nonlinear time-series characteristics of construction carbon emission data, this study incorporates CNN, GRU, and LSTM into the predictive model to enable deeper extraction of carbon emission features. Additionally, the attention mechanism adaptively assigns weights to critical features, further enhancing the model’s prediction accuracy.

3. Aligned with the "dual carbon" policy objectives and the practical requirements of emission reduction in the construction industry, this study utilizes a hybrid deep learning model to simulate medium- and long-term scenarios for provincial-level carbon emissions. By quantitatively assessing the emission reduction effectiveness and peaking timelines under different scenarios, the study provides actionable insights for the development of targeted, region-specific carbon reduction strategies. This approach also

http://www.aloki.hu ● ISSN 1589 1623 (Print) ● ISSN 1785 0037 (Online)
DOI: http://dx.doi.org/10.15666/aeer/2306_1075110774

supports the green transformation and high-quality development of the construction sector.

The remainder of this paper is organized as follows: Section 2 introduces the methods for calculating carbon emissions and their influencing factors. Section 3 presents the construction of the predictive model and the scenario simulations. Section 4 conducts experimental analysis and offers policy recommendations. Section 5 concludes the study.

Calculation methodology and influencing factors

Carbon emission calculation methodology

Carbon emissions in the construction industry can be categorized into direct and indirect emissions (Zhang et al., 2024). Direct emissions refer to the CO_2 released during the combustion of energy sources directly consumed by construction activities, such as coal, coke, fuel oil, diesel, natural gas, gasoline, and kerosene. Indirect emissions, on the other hand, originate from related industries, particularly from the production of construction materials such as cement, steel, timber, glass, and aluminum.

This study employs the IPCC guidelines to calculate construction-related carbon emissions across 30 provinces in China from 1997 to 2021. The carbon emission calculation model for the construction industry is structured as follows:

$$E=E_{dir}+E_{ind}=\frac{44}{12}\sum_{i=1}^{n}C_i\times\alpha_i+\sum_{j=1}^{n}M_j\times\beta_j\times(1-\varepsilon_j) \quad \text{(Eq.1)}$$

where E , E_{dir}, and E_{ind} represent the total carbon emissions of the construction industry, direct carbon emissions, and indirect carbon emissions, respectively. C_i denotes the consumption of the ith energy source. α_i is the carbon emission factor of the ith energy source. M_j represents the consumption of the jth construction material. β_j is the carbon emission factor of the jth construction material. ε_j is the recyclability coefficient of the jth construction material.

The direct carbon emission sources of the construction industry are identified as eight types of energy, including raw coal, gasoline, kerosene, and others (Xu et al., 2024). The standard coal conversion factors and carbon emission factors for each energy type are shown in *Table 1*. Indirect carbon emission sources are identified as construction materials associated with the construction industry, such as glass, timber, and cement. The carbon emission factors and recyclability coefficients for these materials are listed in *Table 2*.

Table 1. *Standard coal conversion factors and carbon emission factors for different energy types*

Energy Type	Raw Coal	Gasoline	Kerosene	Diesel	Fuel Oil	Liquefied Petroleum Gas	Natural Gas	Electricity
Standard Coal Conversion Factor (kgce/kg)	0.7143	1.4714	1.4714	1.4571	1.4286	1.7143	1.3300	0.1229
Carbon Emission Factor (kgCO2/kgce)	0.7559	0.5538	0.5714	0.5921	0.6185	0.5042	0.4483	0.2900

Table 2. *Carbon emission factors and recyclability coefficients for major construction materials*

Construction Material	Cement	Glass	Steel	Aluminum	Timber
Carbon Emission Factor	0.815 kg/kg	0.9655 kg/kg	1.789 kg/kg	2.6 kg/kg	-842.8 kg/kg
Recyclability Coefficient	—	0.7	0.8	0.85	0.2

Selection of influencing factors

The STIRPAT model is an extension and refinement of the IPAT equation, incorporating stochasticity and regression analysis to better accommodate varying data characteristics and uncertainties. It is widely used in environmental science and sustainable development research to analyze the relationships among *P* (population), *A* (affluence), *T* (technology), and *I* (environmental impact). This model provides a scientific foundation for environmental policy formulation and sustainable development strategies.

$$I = a \times P^b \times A^c \times T^d \times e \quad \text{(Eq.2)}$$

where *I* represent the environmental impact. *P*, *A* and *T* denote the population, economic, and technological influencing factors, respectively. *a*, *b*, *c*, and *d* are the parameters to be estimated, reflecting the contributions of each factor to the environmental impact. e is the stochastic error term, capturing other factors and their random fluctuations not accounted for by the model.

To construct the extended STIRPAT model, nine variables were selected as the primary factors influencing carbon emissions in the construction industry, spanning four dimensions: population, economy, technology, and the construction industry. Population factors were represented by total population (P) and urbanization rate (U). The economic factor was represented by Gross Domestic Product (GDP), while the technological factor was measured by energy intensity (CI), defined as energy consumption per unit of GDP. The construction industry dimension included five variables: the number of employees in the construction industry (E), gross output value of the construction industry (GVP), added value of the construction industry (GVA), completed building area (A), and labor productivity in the construction industry (L).

The nine variables selected for the extended STIRPAT model were identified based on a comprehensive consideration of the characteristics of carbon emissions in the construction industry, insights from previous studies, data availability across provinces, and key national development plans and policy targets. This selection enables the model to effectively capture the primary drivers of emissions and the structural dynamics of China’s provincial construction sector.

Considering data availability, the study focused on 30 provinces in China, excluding Tibet, Hong Kong, Macau, and Taiwan, during the period from 1997 to 2021. Data for total population, urbanization rate, and GDP were primarily obtained from the *China Statistical Yearbook*. Energy consumption data were sourced from the *China Energy Statistical Yearbook*, while data on the number of employees, gross output value, completed building area, and labor productivity in the construction industry were extracted from the *China Construction Industry Statistical Yearbook*.

The Pearson correlation analysis was conducted to evaluate the relationship between carbon emissions in the construction industry and the selected influencing factors. The

http://www.aloki.hu ● ISSN 1589 1623 (Print) ● ISSN 1785 0037 (Online)
DOI: http://dx.doi.org/10.15666/aeer/2306_1075110774

results are presented in *Table 3*. The absolute values of the correlation coefficients between construction industry carbon emissions and GDP, gross output *GVP*, added *GVA*, *P*, *E*, *A*, *U*, *L* and *CI* all exceeded 0.8. This indicates a strong correlation between construction industry carbon emissions and the nine selected influencing variables, confirming the appropriateness of these variables for the analysis.

Table 3. *Pearson correlation coefficients for influencing factors*

Variable	*GDP*	*GVP*	*GVA*	*P*	*E*	*A*	*U*	*L*	*CI*
GDP	1								
GVP	.998**	1							
GVA	.999**	.998**	1						
P	.969**	.968**	.960**	1					
E	.964**	.965**	.955**	.982**	1				
A	.926**	.933**	.911**	.975**	.975**	1			
U	.969**	.965**	.958**	.996**	.976**	.963**	1		
L	.989**	.991**	.983**	.983**	.972**	.960**	.981**	1	
CI	-.950**	-.949**	-.937**	-.992**	-.975**	-.981**	-.987**	-.972**	1

Note: Significant at the 0.01 level (two-tailed)

Methods

CNN

Convolutional Neural Networks are typically employed in image processing tasks, but they can also effectively extract local features from time-series data. As illustrated in *Fig. 1*, the basic structure of a CNN typically includes an input layer, convolutional layers, and pooling layers (Liu et al., 2024) A key characteristic of CNNs is their ability to perform local perception through convolutional operations, enabling the network to focus on learning localized patterns.

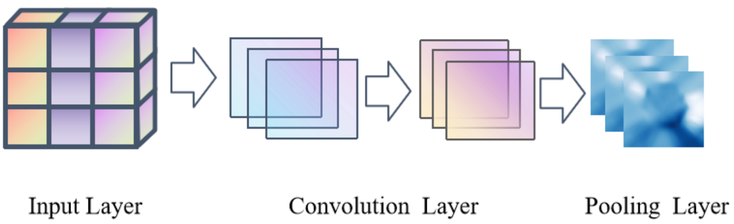

Figure 1. *Structure diagram of CNN*

In this model, CNN is primarily used to perform convolutional operations on the input data, uncovering spatial information and local patterns within the features. By extracting spatial features through multiple convolutional layers, the model can automatically identify critical information in the data, significantly reducing the need for manual feature engineering. This process is particularly effective in handling complex spatiotemporal datasets, where CNNs help the model automatically capture meaningful features from raw input data. The convolutional operation can be represented as:

http://www.aloki.hu ● ISSN 1589 1623 (Print) ● ISSN 1785 0037 (Online)
DOI: http://dx.doi.org/10.15666/aeer/2306_1075110774

$$H_{CNN} = \sigma(W_{CNN} * X + b_{CNN}) \quad \text{(Eq.3)}$$

where W_{CNN} and b_{CNN} denote the convolutional kernel weights and biases, respectively, and σ represents the activation function.

GRU

The Gated Recurrent Unit is a variant of the Recurrent Neural Network (RNN) designed to address the gradient vanishing problem commonly encountered in traditional RNNs when processing long sequence data. As illustrated in *Fig. 2*, GRU introduces mechanisms for an update gate and a reset gate, enabling the selective retention or forgetting of past information to flexibly capture short-term temporal features (Lv et al., 2024).

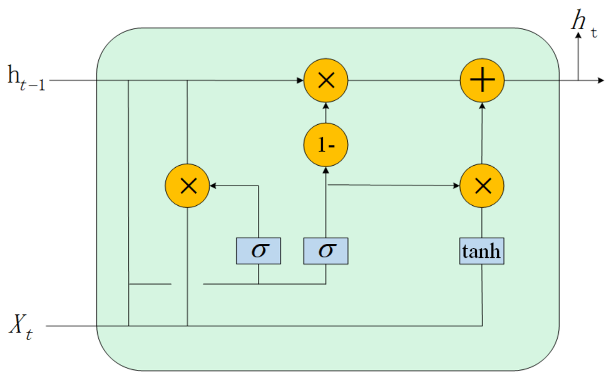

Figure 2. *Structure diagram of GRU network*

In this study, GRU is employed to model the short-term temporal dependencies in construction industry carbon emission data. This is particularly useful in scenarios where factors influencing carbon emissions exhibit significant short-term fluctuations. GRU effectively identifies and tracks these variations, providing a robust solution for short-term modeling. The update equations for GRU are as follows:

$$z_t = \sigma(W_z x_t + U_z h_{t-1}) \quad \text{(Eq.4)}$$

$$r_t = \sigma(W_r x_t + U_r h_{t-1}) \quad \text{(Eq.5)}$$

$$\widetilde{h_t} = tanh\big(W_h x_t + U_h(r_t \odot h_{t-1})\big) \quad \text{(Eq.6)}$$

$$h_t = z_t \odot h_{t-1} + (1 - z_t) \odot \widetilde{h_t} \quad \text{(Eq.7)}$$

where z_t represents the update gate, r_t denotes the reset gate, and $\widetilde{h_t}$ is the hidden state of the GRU.

LSTM

The Long Short-Term Memory network is a specialized architecture of Recurrent Neural Networks designed to learn long-term dependencies while avoiding the gradient vanishing or exploding problems typically encountered with traditional RNNs when

http://www.aloki.hu ● ISSN 1589 1623 (Print) ● ISSN 1785 0037 (Online)
DOI: http://dx.doi.org/10.15666/aeer/2306_1075110774

processing long sequences. As illustrated in *Fig. 3*, LSTM introduces "cell states" and "gating mechanisms," enabling the network to retain and update information selectively, thereby remembering critical past information and discarding irrelevant data (Huang et al., 2024).

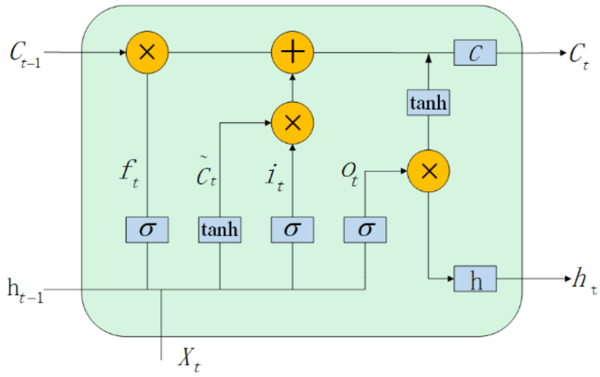

Figure 3. *Structure diagram of LSTM network*

In this study, LSTM is utilized to model the temporal characteristics of carbon emissions in the construction industry. Its ability to effectively handle nonlinear relationships between carbon emissions and input variables makes it particularly advantageous for capturing the complex dependencies in time-series data. The update equations for LSTM are as follows:

$$f_t = \sigma\left(W_f x_t + U_f h_{t-1} + b_f\right) \tag{Eq.8}$$

$$i_t = \sigma(W_i x_t + U_i h_{t-1} + b_i) \tag{Eq.9}$$

$$\widetilde{c_t} = tanh(W_c x_t + U_c h_{t-1} + b_c) \tag{Eq.10}$$

$$c_t = f_t \odot c_{t-1} + i_t \odot \widetilde{c_t} \tag{Eq.11}$$

$$o_t = \sigma(W_o x_t + U_o h_{t-1} + b_o) \tag{Eq.12}$$

$$h_t = o_t \odot tanh(c_t) \tag{Eq.13}$$

where f_t, i_t, and o_t represent the forget gate, input gate, and output gate, respectively. c_t denotes the cell state.

Attention

The attention mechanism, originally developed in the field of natural language processing, enhances a model's ability to "focus" on the most critical parts of an input sequence by assigning weights to different elements. In this model, the attention mechanism is employed to improve the model's ability to concentrate on key input features, effectively weighting their importance across different time steps. This approach allows the model to assign higher significance to critical historical data, thereby enhancing prediction accuracy (Yin et al., 2024).

http://www.aloki.hu ● ISSN 1589 1623 (Print) ● ISSN 1785 0037 (Online)
DOI: http://dx.doi.org/10.15666/aeer/2306_1075110774

When applied to the time-series data of carbon emissions in the construction industry, the attention mechanism helps the model identify which factors have the most substantial impact on carbon emissions at various stages, facilitating a more nuanced understanding of temporal dependencies. The calculations for the attention mechanism are as follows:

$$e_t = v^{\top} tanh(W_e h_t + b_e) \quad \text{(Eq.14)}$$

$$\alpha_t = \frac{exp(e_t)}{\sum_{k=1}^{T} exp(e_k)} \quad \text{(Eq.15)}$$

$$h^* = \sum_{t=1}^{T} \alpha_t h_t \quad \text{(Eq.16)}$$

where e_t represents the importance score of time step t, α_t is the corresponding attention weight, and h^* is the weighted global feature representation.

CNN-GRU-LSTM-Attention model

To enhance the accuracy of carbon emission predictions in the construction industry, this study proposes a composite model integrating CNN, GRU, LSTM, and an attention mechanism (CNN-GRU-LSTM-Attention). This model effectively captures the temporal characteristics, spatial features, and nonlinear relationships inherent in carbon emission data, leveraging the strengths of multiple deep learning methods to improve prediction accuracy and robustness.

As shown in *Fig. 4*, the CNN-GRU-LSTM-Attention model begins with the CNN module, which extracts local spatial features from the input data through convolutional operations. These features are then passed through a pooling layer, which reduces dimensionality and yields a compact feature representation, denoted as X_t. Subsequently, this compact representation is transformed by a fully connected layer, preparing it for temporal modeling.

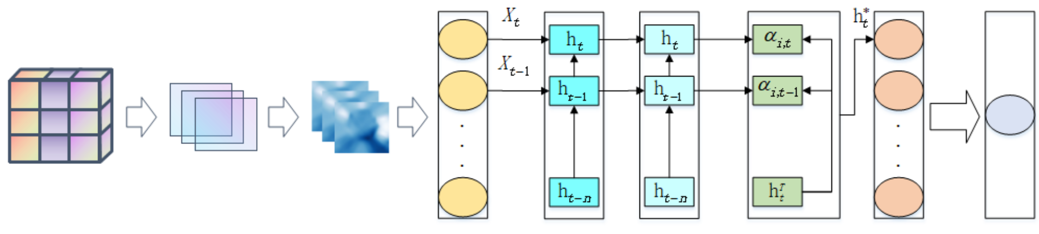

Figure 4. *Structure diagram of CNN-GRU-LSTM-Attention combined model*

Next, the data enters the recurrent neural network module, where the GRU component captures short-term temporal dependencies. By employing update and reset gates, the GRU controls the flow of information, generating a hidden state h_t for each time step. Following this, the LSTM module builds on the GRU outputs to model long-term

http://www.aloki.hu ● ISSN 1589 1623 (Print) ● ISSN 1785 0037 (Online)
DOI: http://dx.doi.org/10.15666/aeer/2306_1075110774

dependencies. Its memory cells retain essential information while the forget and output gates provide fine-grained control over state dynamics.

Afterward, the outputs of the LSTM (h_t) are processed by the attention mechanism, which assigns weights $\alpha_{i,t}$ to different time steps. This step enables the model to emphasize key temporal features and focus on the most influential inputs across time. Finally, the weighted global feature representation h_t^* produced by the attention mechanism is passed through another fully connected layer, where it is further refined to generate the final carbon emission prediction.

Scenario design and parameter settings

This study indirectly incorporates potential future policy changes and technological advancements affecting construction carbon emissions by designing multiple development scenarios.

The prediction of carbon emissions in the construction industry incorporates nine input variables: population, number of employees in the construction industry, GDP, gross output value of the construction industry, added value of the construction industry, urbanization rate, completed building area, labor productivity in the construction industry, and energy intensity. The prediction period spans from 2022 to 2035, divided into three phases: T1 (2022–2025), T2 (2026–2030), and T3 (2031–2035).

Three scenarios were designed (Zhang et al., 2024): baseline, green development, and high-speed development. The baseline scenario assumes that China's energy conservation and emission reduction policies are effectively implemented, reflecting the future trends of carbon emissions in the construction industry under current policy directions. The green development scenario envisions broader adoption of green technologies and significant reductions in energy consumption in alignment with existing economic development plans. In contrast, the high-speed development scenario assumes that economic growth remains the primary focus, with rapid development in both the economy and the construction industry, leading to higher growth rates in energy consumption and coal use.

The growth rates under the three scenarios were established with reference to both historical development trends (1997–2021) and relevant national policies, including the 14th Five-Year Plan and China's dual carbon targets.

The growth rates for nine key indicators under different scenarios across the three periods (T1, T2, T3) are summarized below as shown in *Table 4*.

Table 4. *Predicted growth rates of influencing factors*

Scenario	Period	*P*	*E*	*GDP*	*GVP*	*GVA*	*U*	*A*	*L*	*CI*
Baseline	2022-2025	0.25%	-1.2%	5.42%	9%	4.5%	1.1%	-0.49%	4.5%	-2.7%
	2026-2030	0.05%	-1.3%	4.92%	8%	4%	0.95%	-0.54%	4.3%	-2.5%
	2031-2035	-0.15%	-1.4%	4.48%	7%	3.5%	0.75%	-0.59%	4.1%	-2%
Green	2022-2025	0.15%	-1.7%	4.92%	8%	4%	1.05%	-0.69%	4.3%	-3.7%
	2026-2030	-0.05%	-1.8%	4.42%	7%	3.5%	0.9%	-0.74%	4.1%	-3.5%
	2031-2035	-0.25%	-1.9%	3.98%	6%	3%	0.7%	-0.79%	3.9%	-3%
High-Speed	2022-2025	0.35%	-0.7%	5.92%	10%	5%	1.15%	-0.39%	4.7%	-1.7%
	2026-2030	0.15%	-0.8%	5.42%	9%	4.5%	1%	-0.44%	4.5%	-1.5%
	2031-2035	-0.05%	-0.9%	4.98%	8%	4%	0.8%	-0.49%	4.3%	-1%

http://www.aloki.hu ● ISSN 1589 1623 (Print) ● ISSN 1785 0037 (Online)
DOI: http://dx.doi.org/10.15666/aeer/2306_1075110774

(1) Population (P)

Due to the increasing severity of population aging and shifting fertility norms, China's population growth is expected to slow further. According to the National Population Development Plan (2016–2030) issued by the State Council, China's population was projected to reach 1.42 billion by 2020 and approximately 1.45 billion by 2030. The World Population Prospects (2024) published by the United Nations indicates that China's population will enter a phase of sustained decline, potentially dropping to 1.2 billion by 2050. Based on the findings of Xu et al. (2024), the population growth rates for the baseline scenario are set at 0.25%, 0.05%, and -0.15% for T1, T2, and T3, respectively. The green and high-speed development scenarios assume deviations of ±0.1% from these baseline rates.

(2) Number of employees in the construction industry (E)

With the slowdown in China's economic growth and structural adjustments within the construction sector, the growth rate of employees in the construction industry is expected to decline progressively. According to the 2023 Statistical Analysis of Construction Industry Development published by the China Construction Industry Association, the number of employees in the construction industry has experienced four consecutive years of negative growth since 2019. Additionally, the sector's shift towards intelligent and digitalized operations may lead to the replacement of some traditional labor-intensive roles with automated or technology-intensive positions, further reducing workforce growth rates. Referring to Zhou et al. (2024), the baseline scenario sets growth rates for construction employees at -1.2%, -1.3%, and -1.4% for T1, T2, and T3, respectively. The green and high-speed development scenarios assume deviations of ±0.5% from these baseline rates.

(3) GDP

As China transitions from rapid growth to high-quality development, the national GDP growth rate is expected to decelerate progressively. According to economic development plans issued by the State Council and forecasts by international economic organizations, although China will remain a key player in the global economy, its growth rate will be significantly lower than in the past decade. Official data show that China's GDP was approximately ¥99.1 trillion in 2019, with an expected average annual growth rate of about 5% by 2025. The International Monetary Fund predicts that, amidst global economic uncertainties and a gradually saturated domestic market, China's GDP growth rate will stabilize. By 2050, due to accelerated population aging, a shrinking labor force, and economic restructuring, GDP growth may further decline to around 3%, even though the overall economic scale will continue to expand.

Based on projections from the *China Economic Report* (2020) by the Chinese Academy of Social Sciences, the baseline scenario sets GDP growth rates for T1, T2, and T3 at 5.42%, 4.92%, and 4.48%, respectively. The green and high-speed development scenarios assume deviations of ±0.5% from these baseline rates.

(4) Gross output value of the construction industry (GVP)

According to the National Bureau of Statistics, the gross output value of the construction industry has grown at an average annual rate of 12.9% over the past 70 years. However, during the 13th Five-Year Plan period, this growth rate declined to between 5% and 10%. Despite this slowdown, continuous government investment in infrastructure, urban renewal, and the renovation of aging neighborhoods will sustain growth potential in the construction sector.

http://www.aloki.hu ● ISSN 1589 1623 (Print) ● ISSN 1785 0037 (Online)
DOI: http://dx.doi.org/10.15666/aeer/2306_1075110774

Nonetheless, the labor-intensive nature of the construction industry is expected to diminish gradually as structural adjustments shift the focus toward green, intelligent, and technologically advanced construction projects. Consequently, the growth rate of GVP is anticipated to be slower compared to historical levels.

Under the baseline scenario, growth rates for GVP are set at 9%, 8%, and 7% for T1, T2, and T3, respectively. The green and high-speed development scenarios assume deviations of ±1% from these baseline rates.

(5) Gross value added of the construction industry (GVA)

According to the In-Depth Research and Future Prospects Report on China's Construction Industry Development (2022–2029), the gross value added of the construction industry has maintained consistent growth over the past decade. In 2021, GVA reached approximately ¥8 trillion, a 2.1% increase compared to 2020. During the 13th Five-Year Plan period, significant progress was achieved in the reform and development of the construction sector, with an average annual growth rate of 5.1%. However, as China's economic growth slows and the construction industry shifts towards greener and more intelligent practices, the growth of GVA is expected to stabilize.

Under the baseline scenario, growth rates for GVA are set at 4.5%, 4%, and 3.5% for T1, T2, and T3, respectively. The green and high-speed development scenarios assume deviations of ±0.5% from these baseline rates.

(6) Urbanization rate (U)

According to the targets outlined in the 14th Five-Year Plan, China's urbanization rate among the permanent population is expected to increase to 65% by 2025. This reflects the government’s strategic focus on advancing urbanization, optimizing regional development, and enhancing urbanization levels. Furthermore, the National Population Development Plan (2016–2030) issued by the State Council projects an urbanization rate of 70% by 2030, signifying a new phase of urban development. Research by Qiao et al. (2024) aligns with these projections, estimating that China’s urbanization rate will reach 70% by 2030 and rise further to approximately 80% by 2050.

Based on these studies and Liu et al.’s research (Chunsen et al., 2024), the baseline scenario assumes urbanization growth rates of 1.1%, 0.95%, and 0.75% for T1, T2, and T3, respectively. The green and high-speed development scenarios introduce deviations of ±0.05% from these baseline rates.

(7) Completed building area (A)

With the slowdown in urbanization and the gradual regulation of the real estate market, the growth rate of completed building area is expected to decline progressively. According to the 2023 Statistical Analysis of Construction Industry Development published by the China Construction Industry Association, the growth rate of completed building area has been decreasing annually since 2012, with four consecutive years of negative growth starting from 2017.

Under the baseline scenario, the growth rates of completed building area for T1, T2, and T3 are set at -0.49%, -0.54%, and -0.59%, respectively. For the green development scenario, these rates fluctuate by ±0.2%, while for the high-speed development scenario, they fluctuate by ±0.1%.

(8) Labor productivity in the construction industry (L)

As new technologies such as Building Information Modeling, smart construction, and 3D printing are increasingly adopted, the productivity of the construction industry is anticipated to improve significantly. Green building initiatives and low-carbon technologies will further enhance production methods, reducing reliance on traditional

http://www.aloki.hu ● ISSN 1589 1623 (Print) ● ISSN 1785 0037 (Online)
DOI: http://dx.doi.org/10.15666/aeer/2306_1075110774

labor. According to the 2023 Statistical Analysis of Construction Industry Development, the labor productivity of construction enterprises in 2022 was 1.52 times that of 2013, with an average annual growth rate of 4.76% over the decade. However, the annual growth rate decreased from 9.59% in 2013 to 4.3% in 2022, marking a decline of 5.29 percentage points.

In the baseline scenario, the growth rates of labor productivity for T1, T2, and T3 are set at 4.5%, 4.3%, and 4.1%, respectively. These rates fluctuate by ±0.2% in both the green and high-speed development scenarios.

(9) Energy intensity (CI)

According to the Action Plan for Reaching Carbon Peak Before 2030 and the 14th Five-Year Comprehensive Work Plan for Energy Conservation issued by the State Council, China aims to reduce energy consumption per unit of GDP by 13.5% by 2025 compared to 2020 levels. This target reflects the nation's determination to advance the transition to a green and low-carbon economy, a critical step toward achieving carbon peak goals. Additionally, the Energy and Power Development Plan for China 2030 and 2060 Outlook published by the Global Energy Interconnection Development and Cooperation Organization predicts that China's energy demand will peak at 5.6 billion tons of standard coal by 2025 and 6 billion tons by 2030, reaching its highest level before 2035.

With the ongoing transformation and upgrading of China's economy, energy intensity is expected to continue declining. Under the baseline scenario, the growth rates of energy intensity for T1, T2, and T3 are set at -2.7%, -2.5%, and -2%, respectively. For the green and high-speed development scenarios, these rates fluctuate by ±1%.

Experimental results

Prediction results of different models

The input data for the models consists of construction-related carbon emission influencing factors from 30 provinces in China, spanning the years 1997 to 2021. The output is the predicted CO_2 emissions. The 25-year dataset for each province is divided into training and testing sets, with the first 20 years (600 samples) used for training and the last 5 years (150 samples) used for testing. In the prediction phase, the input variables were modified according to the assumptions of the three development scenarios, ensuring that the scenario projections were directly embedded in the modeling process.

In this study, China's 31 provincial-level administrative regions were treated as independent spatial units. Each province was modeled separately by inputting its respective construction-related features into a unified prediction framework. Although spatial econometric techniques such as spatial autocorrelation or spatial weight matrices were not explicitly applied, the model was able to learn and capture regional heterogeneity in carbon emissions through province-specific input data.

The input layer of the model is a sequence input layer, which receives the processed dataset and maps it into a format suitable for network processing. Each input sample is a time series of nine features, with a time window of one. The convolutional component consists of two convolutional layers: the first with 32 channels and the second with 128 channels. After feature extraction, the model incorporates an attention mechanism. First, a global average pooling layer summarizes the features extracted by the convolutional layers. Then, two fully connected layers weight the extracted features, and the weights are normalized using a sigmoid layer. These weights are multiplied with the convolutional

http://www.aloki.hu ● ISSN 1589 1623 (Print) ● ISSN 1785 0037 (Online)
DOI: http://dx.doi.org/10.15666/aeer/2306_1075110774

features, enhancing the model's focus on critical features and improving prediction performance.

Subsequently, GRU and LSTM layers are used to capture the long-term dependencies in the time-series data. The GRU layer, with 64 neurons, extracts the temporal dependencies of carbon emission data, identifying short- and mid-term temporal patterns. The LSTM layer, with 15 neurons, refines the GRU output by further capturing long-term trends, enabling more accurate predictions of the complex variations in construction industry carbon emissions. Finally, the model outputs the predictions through a fully connected layer and a regression layer, providing the final carbon emission forecasts.

During training, the Adam optimizer is used, with an initial learning rate set to 0.005. The maximum number of iterations is set to 50, and a learning rate scheduling strategy reduces the learning rate every 25 epochs. The model is trained using a batch size of 32, and time-series data is unfolded and folded to optimize the model's ability to learn sequential patterns.

To evaluate the prediction performance of different models for construction industry carbon emissions, comparisons were made among the LSTM, CNN-GRU-LSTM, and CNN-GRU-LSTM-Attention models. Scatter plots and error diagrams for the predictions of the three models are shown in *Fig. 5* and *Fig. 6*. Additionally, three error metrics, Root Mean Square Error (RMSE), Mean Absolute Error (MAE), and Mean Absolute Percentage Error (MAPE), were used to assess the predictive accuracy of each model. The comparison results are presented in *Table 5*.

$$RMSE = \sqrt{\frac{1}{N}\sum_{i=1}^{N} (y_i - \hat{y}_i)^2} \quad \text{(Eq.17)}$$

$$MAE = \frac{1}{N}\sum_{i=1}^{N} |y_i - \hat{y}_i| \quad \text{(Eq.18)}$$

$$MAPE = \frac{100\%}{N}\sum_{i=1}^{N} \left|\frac{y_i - \hat{y}_i}{y_i}\right| \quad \text{(Eq.19)}$$

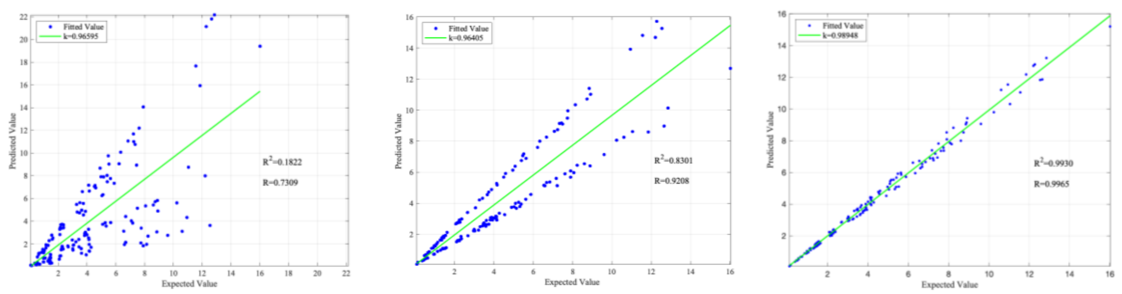

(a) LSTM (b) CNN-GRU-LSTM (c) CNN-GRU-LSTM-Attention

Figure 5. *Scatter plot illustrating the fitting results of different models*

http://www.aloki.hu ● ISSN 1589 1623 (Print) ● ISSN 1785 0037 (Online)
DOI: http://dx.doi.org/10.15666/aeer/2306_1075110774

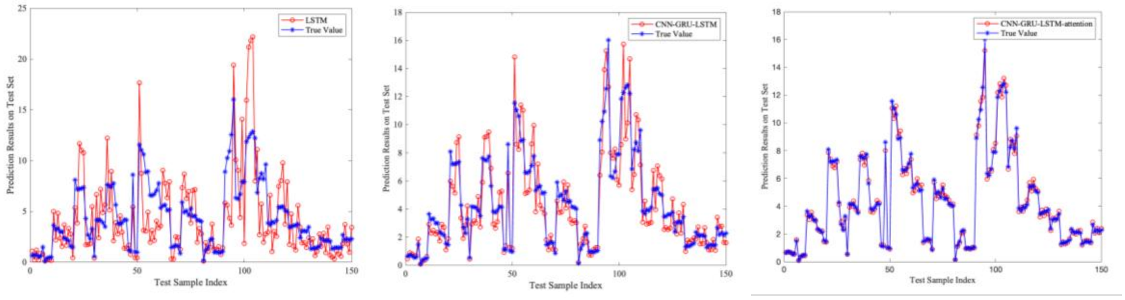

(a) LSTM (b) CNN-GRU-LSTM (c) CNN-GRU-LSTM-Attention

Figure 6. *Error plot showing the prediction errors for different models*

Table 5. *Error metrics for different models*

Error Metric	LSTM	CNN-GRU-LSTM	CNN-GRU-LSTM-Attention
RMSE	2.9681	1.3528	0.27508
MAE	2.1996	1.0915	0.2134
MAPE (%)	50.6535	24.4268	4.7285

Based on *Fig. 5* and *Fig. 6* and the results in *Table 5*, it is evident that the RMSE, MAE, and MAPE of the LSTM and CNN-GRU-LSTM models are consistently higher than those of the CNN-GRU-LSTM-Attention model. Additionally, the CNN-GRU-LSTM-Attention model achieves an R^2 value of 0.993, which is significantly higher than the R^2 values of the other two models. This indicates that the CNN-GRU-LSTM-Attention model is highly effective in fitting the relationships between the influencing factors and carbon emissions.

In summary, the CNN-GRU-LSTM-Attention model demonstrates superior predictive accuracy and robustness, providing a reliable foundation for forecasting construction industry carbon emissions under various scenarios.

National carbon emission trends in the construction industry

Fig. 7 illustrates the historical and projected trends of carbon emissions in China's construction industry under different scenarios. The period from 1997 to 2021 represents historical carbon emission data, while 2022 to 2035 reflects predicted values under varying development scenarios. The figure shows that the goal of peaking carbon emissions in the construction industry before 2030 is achievable.

The historical data indicate a continuous increase in carbon emissions since 1997, with an accelerated growth rate after 2010. This surge reflects the intensification of construction activities and energy consumption, likely driven by rapid urbanization, increased building demand, and industrialization.

Under the baseline and green development scenarios, carbon emissions peaked earlier, in 2019, at approximately 140 million tons. In contrast, the high-speed development scenario, which assumes rapid economic and construction sector growth, predicts a delayed peak in 2026 at 143 million tons. Moreover, the decline in emissions under this scenario is notably slower.

http://www.aloki.hu ● ISSN 1589 1623 (Print) ● ISSN 1785 0037 (Online)
DOI: http://dx.doi.org/10.15666/aeer/2306_1075110774

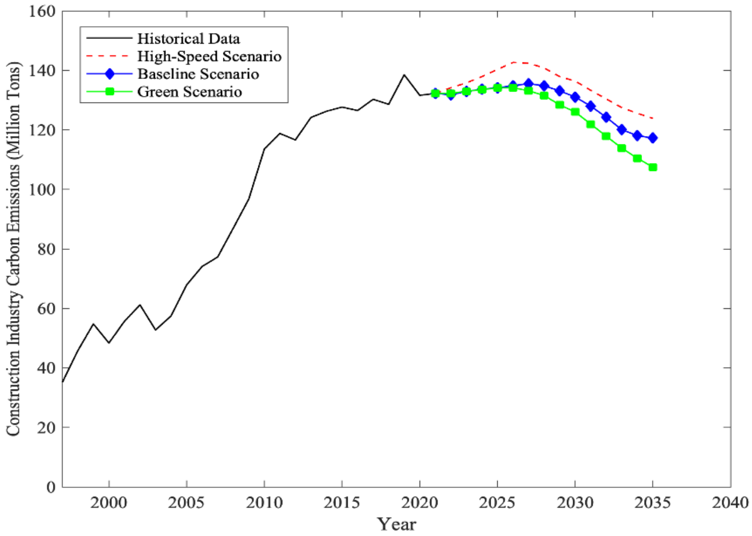

***Figure 7.** National carbon peaking pathways under different scenarios*

The variations in peak timing and peak levels across scenarios highlight the significant impact of policy and technological interventions on controlling carbon emissions. The green development scenario demonstrates that measures such as optimizing the energy mix and promoting green buildings can effectively reduce the carbon emission peak and accelerate the decline in emissions. Meanwhile, the high-speed scenario underscores the challenges of controlling emissions amid rapid economic growth, signaling the need for heightened attention from policymakers.

Regional carbon emissions in the construction industry

Based on the projections for 30 provinces in China under different scenarios shown in Appendix A, this section analyzes the results from three perspectives: historical trends, future scenario predictions, and regional differences within the overall trajectory.

Provinces that peaked later under the baseline and high-speed development scenarios but achieved significantly earlier peaks and larger emission reductions under the green development scenario were identified as having high emission reduction potential. This classification reflects both their stronger responsiveness to low-carbon development strategies and their greater capacity for structural transition in the construction sector.

(a) Historical trend analysis

An analysis of the historical carbon emission trends from 1997 to 2021 indicates that all 30 provinces are expected to achieve carbon peaking in the construction industry before 2030. However, significant regional disparities and phased characteristics can be observed in the evolution of construction-related carbon emissions across provinces.

In general, the characteristics of carbon emission changes in each province can be summarized as regions where carbon emissions have already peaked and are declining, and regions where carbon emissions are still increasing. Provinces in Northeast China, North China, and most of the Eastern region have seen their construction industry carbon emissions peak during the study period, followed by a significant downward trend. These provinces are mainly concentrated in economically developed regions or areas that have taken the lead in promoting the transformation and upgrading of the construction industry.

http://www.aloki.hu ● ISSN 1589 1623 (Print) ● ISSN 1785 0037 (Online)
DOI: http://dx.doi.org/10.15666/aeer/2306_1075110774

The decline can likely be attributed to economic restructuring, reduced construction activities, and population outflows.

In contrast, some provinces in the Central and Western regions, such as Sichuan, Chongqing, and Guangxi, have shown continuous growth in construction-related carbon emissions during the study period and have not yet peaked. These provinces are typically driven by accelerated urbanization and increased demand for infrastructure development. The continued growth in construction industry carbon emissions indicates that these regions are still in the expansion phase of their construction industries, with economic development and urbanization being important drivers of carbon emissions. Balancing development and emission reductions will become a key challenge for these regions in the future.

(b) Future scenario prediction analysis

Under the high-speed development scenario, although some provinces maintain certain emission growth in the short term, emissions eventually exhibit a declining trend after peaking. However, the rate of increase and the peak emission levels vary across provinces. Most provinces reach their highest emission levels under this scenario, reflecting the significant impact of rapid economic growth on construction-related emissions. Provinces such as Sichuan, Chongqing, Henan, Guangxi, Hainan, Guizhou, and Qinghai experience relatively delayed carbon emission peaks under the high-speed development scenario. This indicates a stronger dependence of the construction industry on economic growth in these regions, leading to a later transition to the emission reduction phase.

In contrast, provinces such as Tianjin, Guangdong, and Shanxi, despite achieving relatively high carbon emission levels under the high-speed scenario, do not exhibit significantly delayed peak years. This suggests a certain degree of policy regulation and industrial transformation capability in these regions.

Under the baseline scenario, most provinces reach their carbon emission peaks earlier than in the high-speed scenario and gradually transition to a stable or slowly declining phase post-peak. Carbon emissions under this scenario show moderate growth followed by a decline, with most provinces peaking around 2025 and gradually entering the emission reduction phase after 2030.

The green development scenario exhibits the fastest decline in carbon emissions across all provinces, fully reflecting the effectiveness of green technology applications and policy-driven emission reduction efforts. This scenario demonstrates the most favorable emission reduction outcomes, with all provinces achieving significant reductions before 2030, and the peak years for most provinces advancing to around 2025. Provinces in central and western regions, such as Henan, Hunan, Yunnan, and Chongqing, achieve the largest reductions under the green scenario, potentially due to the proactive adoption of low-carbon technologies and benefits from policy support and energy structure optimization.

Economically developed provinces and traditional industrial regions, such as Jiangsu, Zhejiang, Shandong, Fujian, Jiangxi, and Inner Mongolia, display relatively steady declines under all three scenarios. This stability reflects the consistency and continuity of emission reduction policy implementation in these regions.

(c) Regional comparison and overall trend analysis

The high-speed development scenario, while driving rapid economic growth, also results in a significant increase in carbon emission levels, particularly in provinces heavily reliant on the construction industry. In contrast, under the baseline scenario, most

http://www.aloki.hu ● ISSN 1589 1623 (Print) ● ISSN 1785 0037 (Online)
DOI: http://dx.doi.org/10.15666/aeer/2306_1075110774

provinces achieve earlier carbon peaks and gradually transition into a stable decline phase, indicating that construction industry emissions are manageable under moderate development conditions. The green development scenario emerges as the optimal pathway for achieving carbon peaking and carbon neutrality goals.

In the central and western regions, such as Sichuan, Guizhou, Chongqing, and Yunnan, there is notable potential for emission reduction. Under the green development scenario, these provinces achieve significant reductions in carbon emissions, with earlier peak years, demonstrating their substantial capacity for emission control.

In traditional industrial regions such as the Beijing-Tianjin-Hebei area, the Yangtze River Delta, and Northeast China—represented by provinces like Beijing, Jiangsu, Liaoning, and Heilongjiang—a relatively steady decline in carbon emissions is observed across all three scenarios. This indicates that these regions have reached a relatively mature stage in emission reduction, with economic development and carbon mitigation policies advancing in tandem.

Policy recommendations

Based on the projected carbon emissions of the construction industry across 30 Chinese provinces under different development scenarios, the following policy recommendations are proposed to achieve carbon peaking and neutrality targets while promoting coordinated regional development:

(a) Policy recommendations based on empirical findings

(1) Tailor region-specific policies to local conditions: Central and western provinces such as Henan, Hunan, Yunnan, Chongqing, and Guizhou show substantial emission reduction potential under the green development scenario. These regions should accelerate the development and application of green building technologies and improve energy efficiency. In traditional industrial regions like Beijing-Tianjin-Hebei, the Yangtze River Delta, and Northeast China, where emissions are relatively stable, efforts should focus on strengthening the enforcement of energy-saving policies and promoting green retrofitting of aging buildings.

(2) Increase green investment to enhance long-term mitigation capacity: The marked emission reductions under the green development scenario highlight the role of green investment in unlocking mitigation potential. Policies should further promote the implementation of green building standards and increase the proportion of certified green buildings.

(b) Recommendations based on industry trends and literature insights

(1) Advance low-carbon and intelligent transformation in the construction sector: Encourage collaboration between enterprises and research institutions, and support R&D in key areas such as low-carbon materials, energy-efficient construction methods, and reuse of construction waste. Promote the wider application of intelligent technologies such as BIM and AI in building design and construction.

(2) Incorporate the construction sector into the national carbon trading system: Introduce the construction industry into the national emissions trading scheme, establish enterprise-level carbon quotas, and use market mechanisms to incentivize emission reductions by high-emitting firms.

(3) Strengthen carbon emission monitoring and performance evaluation systems: Develop unified accounting standards and dynamic monitoring systems for construction-related emissions. Encourage provinces to establish performance evaluation frameworks to support targeted regulation and timely policy adjustments.

http://www.aloki.hu ● ISSN 1589 1623 (Print) ● ISSN 1785 0037 (Online)
DOI: http://dx.doi.org/10.15666/aeer/2306_1075110774

(c) Strengthen policy and market integration and enhance carbon emission management and monitoring systems

(1) Use financial subsidies and tax incentives to encourage companies to adopt energy-saving technologies and materials in construction processes, advancing the low-carbon transition of the construction industry.

(2) Incorporate the construction sector into the national carbon emissions trading market, establish a carbon quota system for construction enterprises, and encourage high-emission companies to achieve reduction targets through carbon trading.

(3) Develop a nationwide carbon emission monitoring system for the construction industry to enable dynamic monitoring of provincial emission levels, providing timely data support for policy adjustments.

(4) Standardize carbon accounting methods for the construction industry and establish a provincial performance evaluation system for construction-related carbon emissions. Encourage local governments to actively engage in carbon reduction efforts, strengthen regulation of high-energy-consuming and high-emission activities in the construction sector, and promote earlier carbon peaking.

Discussion

The proposed CNN-GRU-LSTM-Attention model offers significant advantages over traditional prediction methods in terms of accuracy and feature representation. The CNN component effectively captures local spatial features and variable interactions; GRU and LSTM layers enhance the model's ability to learn both short- and long-term temporal dependencies; and the attention mechanism selectively emphasizes important time steps or variables. This hybrid structure enables the model to process complex non-linear patterns in carbon emission data more efficiently.

The prediction results of this study are subject to certain uncertainties, primarily due to limitations in data quality, assumptions about future socioeconomic development scenarios, and simplifications within the model itself. Although the data were sourced from authoritative channels, potential statistical errors and missing values remain. Scenario assumptions may be affected by policy changes and technological progress. Additionally, the model does not fully capture complex causal relationships and regional policy differences. Future research could improve prediction accuracy and reliability by enhancing data quality, incorporating more dynamic factors, and including spatial correlation analyses.

Conclusion

This study develops a prediction model based on the CNN-GRU-LSTM-Attention mechanism, utilizing carbon emission data from China's construction industry and nine key influencing factors. The proposed model significantly enhances the accuracy and reliability of carbon emission forecasting. From a global perspective, this research systematically analyzes the spatiotemporal evolution of construction-related carbon emissions, providing valuable insights and practical guidance toward achieving carbon peaking and carbon neutrality goals in the construction industry.

The findings not only validate the effectiveness of the proposed model but also offer a scientific basis for future scenario predictions and policy formulation related to construction industry carbon emissions. By analyzing carbon emission trends under

http://www.aloki.hu ● ISSN 1589 1623 (Print) ● ISSN 1785 0037 (Online)
DOI: http://dx.doi.org/10.15666/aeer/2306_1075110774

baseline, green development, and high-speed development scenarios, this study reveals the spatial heterogeneity of carbon peaking times and emission characteristics across China and its provinces. The results demonstrate that scenario settings significantly impact emission trends. Under the green development scenario, all provinces exhibit notable emission reductions, achieving the most effective outcomes. In contrast, the high-speed development scenario delays carbon peaking in certain provinces and results in the highest overall emission levels.

At the regional level, traditional industrial areas such as Beijing-Tianjin-Hebei, the Yangtze River Delta, and Northeast China show relatively stable carbon emission trends across all scenarios. In contrast, provinces in central, western, and southwestern regions experience greater variations, indicating higher potential for emission reduction and opportunities for policy optimization.

This study provides robust data support and theoretical foundations for scenario-based analysis and future trend forecasting of construction-related carbon emissions. It also serves as a reference for formulating region-specific low-carbon development policies. However, some limitations remain. For instance, the prediction model does not account for potential extreme policy interventions or technological breakthroughs, and certain data inputs may carry uncertainties. These limitations will be addressed in future research.

REFERENCES

[1] Chen, C., Guo, J., Zhang, L., Wu, X., Yang, Z. (2024): Robust multi-scale time series prediction for building carbon emissions with explainable deep learning. – Energy and Buildings 312: 114159.

[2] Chunsen, L., Jiansheng, Q., Yujie, G. (2023): LSTM Model-based Prediction of Carbon Emissions from China's Transportation Sector. – China Environmental Science 43(05): 2574-2582.

[3] Cooray, A., Özmen, I. (2024): Institutions and carbon emissions: an investigation employing STIRPAT and machine learning methods. – Empirical Economics 67(3): 1015-1044.

[4] Ding, Q., Xiao, X., Kong, D. (2023): Estimating energy-related CO2 emissions using a novel multivariable fuzzy grey model with time-delay and interaction effect characteristics. – Energy 263: 126005.

[5] Giannelos, S., Bellizio, F., Strbac, G., Zhang, T. (2024): Machine learning approaches for predictions of CO2 emissions in the building sector. – Electric Power Systems Research 235: 110735.

[6] Hu, Y., Man, Y. (2023): Energy consumption and carbon emissions forecasting for industrial processes: Status, challenges and perspectives. – Renewable and Sustainable Energy Reviews 182: 113405.

[7] Huang, Y., Shen, L., Liu, H. (2019): Grey relational analysis, principal component analysis and forecasting of carbon emissions based on long short-term memory in China. – Journal of Cleaner Production 209: 415-423.

[8] Jiang, P., Gong, X., Yang, Y., Tang, K., Zhao, Y., Liu, S., Liu, L. (2023): Research on spatial and temporal differences of carbon emissions and influencing factors in eight economic regions of China based on LMDI model. – Scientific Reports 13(1): 7965.

[9] Jiang, X. (2024): Prediction method of carbon emissions of intelligent buildings based on secondary decomposition BAS-LSTM. – Clean Technologies and Environmental Policy 27: 1903-1913.

[10] Jin, Y., Sharifi, A., Li, Z., Chen, S., Zeng, S., Zhao, S. (2024): Carbon emission prediction models: A review. – Science of The Total Environment 927: 172319.

http://www.aloki.hu ● ISSN 1589 1623 (Print) ● ISSN 1785 0037 (Online)
DOI: http://dx.doi.org/10.15666/aeer/2306_1075110774

[11] Li, R., You, K., Cai, W., Wang, J., Liu, Y., Yu, Y. (2023): Will the southward center of gravity migration of population, floor area, and building energy consumption facilitate building carbon emission reduction in China? – Building and Environment 242: 110576.
[12] Li, R., Han, X., Wang, Q. (2023): Do technical differences lead to a widening gap in China's regional carbon emissions efficiency? Evidence from a combination of LMDI and PDA approach. – Renewable and Sustainable Energy Reviews 182: 113361.
[13] Li, W. K., Wen, H. X., Nie, P. Y. (2023): Prediction of China's industrial carbon peak: Based on GDIM-MC model and LSTM-NN model. – Energy Strategy Reviews 50: 101240.
[14] Li, X., Lin, C., Lin, M., Jim, C. Y. (2024): Drivers and spatial patterns of carbon emissions from residential buildings: An empirical analysis of Fuzhou city (China). – Building and Environment 257: 111534.
[15] Lin, Y., Ma, L., Li, Z., Ni, W. (2023): The carbon reduction potential by improving technical efficiency from energy sources to final services in China: An extended Kaya identity analysis. – Energy 263: 125963.
[16] Liu, X., Cifuentes-Faura, J., Zhao, S., Wang, L. (2023): Government environmental attention and carbon emissions governance: Firm-level evidence from China. – Economic Analysis and Policy 80: 121-142.
[17] Liu, W., Mao, Z. (2024): Short-term photovoltaic power forecasting with feature extraction and attention mechanisms. – Renewable Energy 226: 120437.
[18] Luo, G., Baležentis, T., Zeng, S. (2023): Per capita CO2 emission inequality of China's urban and rural residential energy consumption: a Kaya-Theil decomposition. – Journal of Environmental Management 331: 117265.
[19] Luo, X., Zhang, Y., Song, Z. (2025): Analysis of carbon emission characteristics and establishment of prediction models for residential and office buildings in China. – Building and Environment 267: 112208.
[20] Lv, Z., Wang, N., Lou, R., Tian, Y., Guizani, M. (2023): Towards carbon Neutrality: Prediction of wave energy based on improved GRU in Maritime transportation. – Applied Energy 331: 120394.
[21] Qiao, W., Li, L., Guan, W., Wang, X., Wang, X. (2018): Prediction of urbanization level in China: 2016-2050. – Economic Geography 38(2): 51-58.
[22] Shaheen, A., Sheng, J., Arshad, S., Muhammad, H., Salam, S. (2025): Forecasting the determinants of environmental degradation: a gray modeling approach. – Energy Sources Part A: Recovery, Utilization, and Environmental Effects 47(1): 1084-1104.
[23] Tian, L., Chai, J., Zhang, X., Pan, Y. (2024): Spatiotemporal evolution and driving factors of China's carbon footprint pressure: Based on vegetation carbon sequestration and LMDI decomposition. – Energy 310: 133299.
[24] Wang, Y., Pan, W. (2023): The contribution of cleaner production in the material industry to reducing embodied energy and emissions in China's building sector. – Building and Environment 242: 110555.
[25] Xiao, Y., Huang, H., Qian, X. M., Zhang, L. Y., An, B. W. (2023): Can new-type urbanization reduce urban building carbon emissions? New evidence from China. – Sustainable Cities and Society 90: 104410.
[26] Xu, Y., Song, W. (2019): Carbon emission prediction of construction industry based on fcs-svm. – Ecol. Econ. 35: 37-41.
[27] Xu, G., Schwarz, P., Yang, H. (2019): Determining China's CO2 emissions peak with a dynamic nonlinear artificial neural network approach and scenario analysis. – Energy Policy 128: 752-762.
[28] Yang, L., Hongyu, C. (2025): Research on factors influencing total carbon emissions of construction based on structural equation modeling: A case study from China. – Building and Environment 275: 112396.
[29] Yin, H., Yin, Y., Li, H., Zhu, J., Xian, Z., Tang, Y., Xiao, L., Rong, J., Li, C., Zhang, H., Xie, Z., Meng, A. (2025): Carbon emissions trading price forecasting based on temporal-

http://www.aloki.hu ● ISSN 1589 1623 (Print) ● ISSN 1785 0037 (Online)
DOI: http://dx.doi.org/10.15666/aeer/2306_1075110774

spatial multidimensional collaborative attention network and segment imbalance regression. – Applied Energy 377: 124357.
[30] Zhang, Z., Liu, R. (2013): Carbon emissions in the construction sector based on input-output analyses. – Journal of Tsinghua University Science and Technology 53(1): 53-57.
[31] Zhang, X., Zhang, D. (2023): Urban carbon emission scenario prediction and multi-objective land use optimization strategy under carbon emission constraints. – Journal of Cleaner Production 430: 139684.
[32] Zhang, G. T., Wang, T., Lou, X. Y., Guan, Z., Zheng, H., Li, Q. (2023): Research on China's provincial carbon emission peak path based on a LSTM neural network approach. – Chin. J. Manag. Sci.
[33] Zhang, W., Xu, Y., Streets, D. G., Wang, C. (2025): Measurement of urbanization and its spatiotemporal heterogenous effects on carbon emission from district heating industry in China. – Energy and Buildings 328: 115182.
[34] Zheng, L., Mueller, M., Luo, C., Yan, X. (2024): Predicting whole-life carbon emissions for buildings using different machine learning algorithms: A case study on typical residential properties in Cornwall, UK. – Applied Energy 357: 122472.
[35] Zhou, W., Cao, X., Dong, X., Zhen, X. (2023): The effects of carbon-related news on carbon emissions and carbon transfer from a global perspective: Evidence from an extended STIRPAT model. – Journal of Cleaner Production 425: 138974.
[36] Zhou, Z., Yu, L., Wang, Y., Tian, Y., Li, X. (2024): Innovative approach to daily carbon dioxide emission forecast based on ensemble of quantile regression and attention BILSTM. – Journal of Cleaner Production 460: 142605.
[37] Zhou, X. H., Hu, P. C., Cheng, P. F. (2025): Carbon Emission Accounting and Peak Carbon Prediction of China's Construction Industry from a Whole Life Cycle Perspective. – Huan Jing Ke Xue 46(4): 2020-2034.

APPENDIX

Appendix A. *Carbon peaking pathways under different scenarios for 30 provinces*

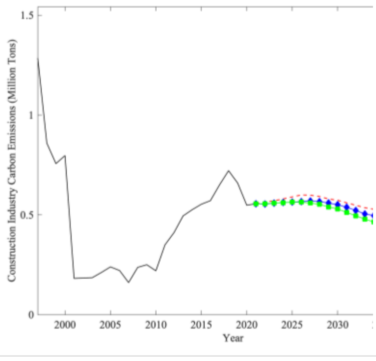

(1) Heilongjiang

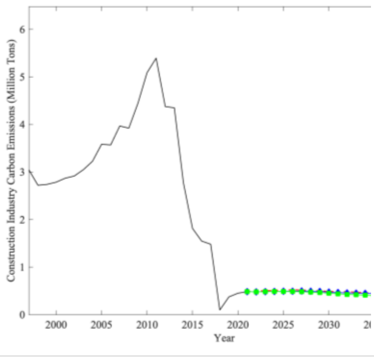

(2) Liaoning

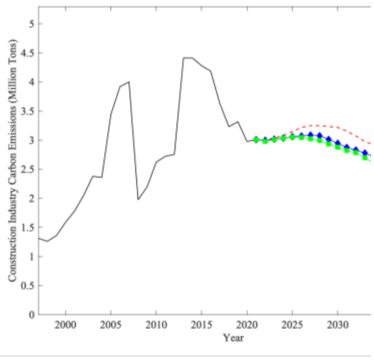

(3) Jilin

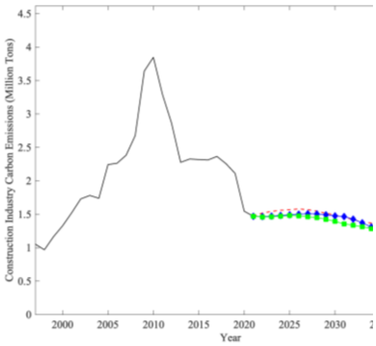

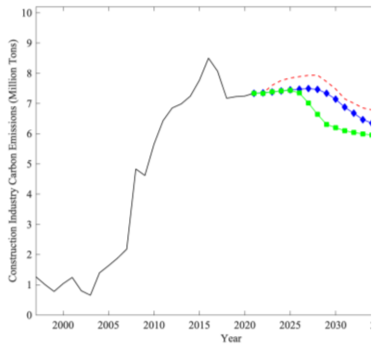

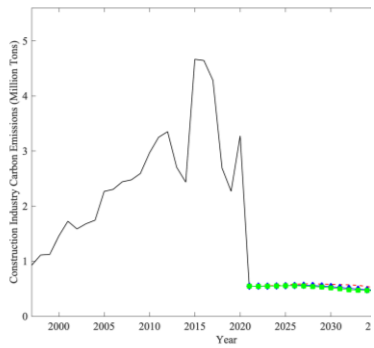

http://www.aloki.hu ● ISSN 1589 1623 (Print) ● ISSN 1785 0037 (Online)
DOI: http://dx.doi.org/10.15666/aeer/2306_1075110774

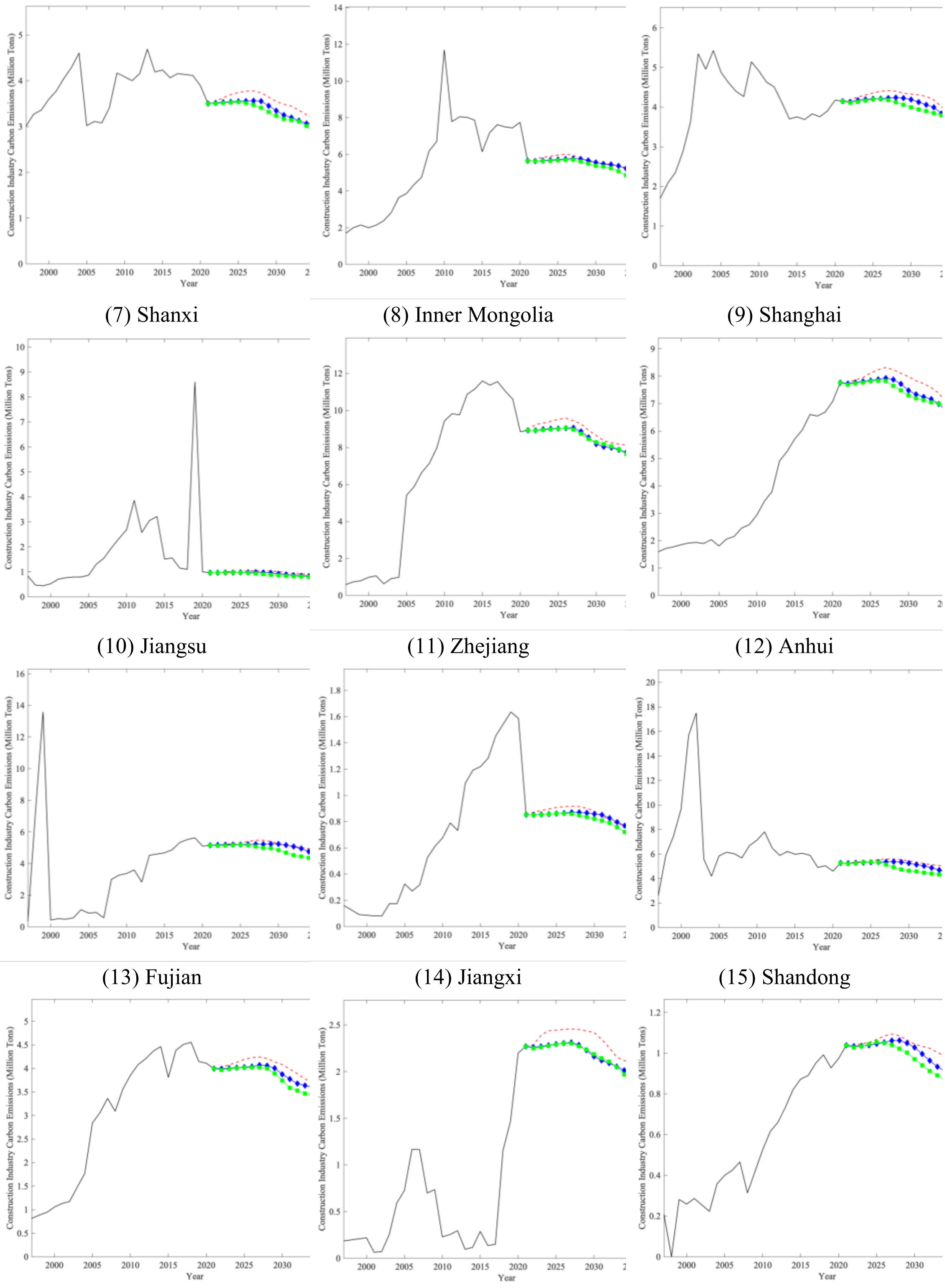

(4) Beijing (5) Tianjin (6) Hebei

(7) Shanxi (8) Inner Mongolia (9) Shanghai

(10) Jiangsu (11) Zhejiang (12) Anhui

(13) Fujian (14) Jiangxi (15) Shandong

(16) Guangdong (17) Guangxi (18) Hainan

http://www.aloki.hu ● ISSN 1589 1623 (Print) ● ISSN 1785 0037 (Online)
DOI: http://dx.doi.org/10.15666/aeer/2306_1075110774

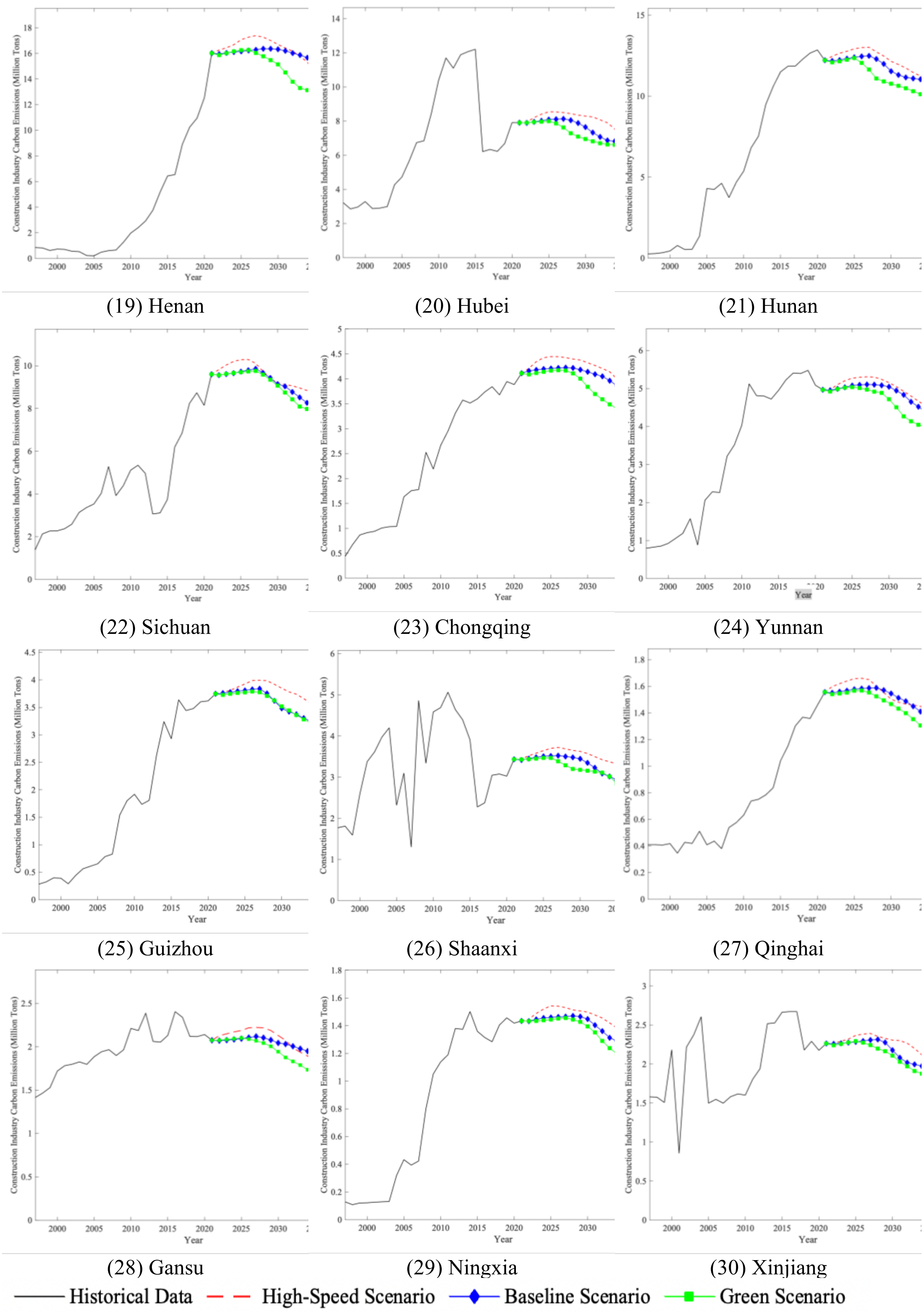
Construction Industry Carbon Emissions (Million Tons)
Year
(19) Henan
(20) Hubei
(21) Hunan
(22) Sichuan
(23) Chongqing
(24) Yunnan
(25) Guizhou
(26) Shaanxi
(27) Qinghai
(28) Gansu
(29) Ningxia
(30) Xinjiang
Historical Data
High-Speed Scenario
Baseline Scenario
Green Scenario